SYNTHETIC PHOTOMETRY AND THE CALIBRATION OF THE HUBBLE SPACE TELESCOPE

J. Koornneef*, R. Bohlin, R. Buser†, K. Horne, D. Turnshek
Space Telescope Science Institute
3700 San Martin Drive
Baltimore, Maryland 21218
U.S.A.

ABSTRACT. The combined Scientific Instruments (SIs) on the Hubble Space Telescope (HST) feature an extensive wavelength coverage in both photometric and spectrophotometric modes with an overall dynamic range of more than twenty-five magnitudes. We demonstrate how synthetic photometry techniques are to be used to establish and maintain their calibration. This approach makes efficient use of limited HST observing time by taking full advantage of pre-launch knowledge on the SI sensitivity functions and calibration targets.

1. INTRODUCTION

One of the responsibilities of the Space Telescope Science Institute (STScI) is to coordinate and maintain the calibration of all the SIs and the Fine Guidance Sensors (FGSs) onboard HST. In the area of photometry and spectrophotometry, this involves dispersed modes on the Faint Object Spectrograph (FOS), the High Resolution Spectrograph (HRS), the Faint Object Camera (FOC), and the Wide Field and Planetary Camera (WFPC), and a total of about 120 filters on the High Speed Photometer (HSP), the WFPC, and the FOC. The SIs are designed to provide complementary capabilities, so that there is limited overlap in dynamic range, spectral coverage and spectral resolution. The calibration of all these observing modes requires an integrated and self-consistent approach which treats the broadband photometric and spectrophotometric measurements in a uniform manner. In Section 2 we develop such a concept, which we will refer to as the *'HST photometric system'*. Section 3 explains how synthetic photometry techniques need to be used to derive instrument-specific calibration data for HST calibration targets from pre-launch information. In Section 4, we show some simulated measurements in the HST photometric system and comment in detail on the effect of passband differences through comparison with a synthetic $(U-B)$,$(B-V)$ diagram.

* Affiliated to the Astrophysics Division, Space Science Department, European Space Agency
† On leave from the Astronomical Institute, University of Basel (Switzerland)

J.-P. Swings (ed.), Highlights of Astronomy, 833–843.

2. DEFINITION OF THE HST PHOTOMETRIC SYSTEM

The HST, like a ground-based photometer, will require a network of calibration targets with known flux distributions to determine the instrument- and mode-specific sensitivity functions. The selection of optical and UV standards for HST has been described by Koornneef *et al.* (1984) and Bohlin *et al.* (1984), respectively.

In the optical regime from 3200 to 10000 Å, absolute flux distributions for a set of *primary* HST spectrophotometric standards (Koornneef *et al.* 1984) are being prepared by J. B. Oke. The *primary* HST spectrophotometric standards for the UV are being prepared by R. C. Bohlin and collaborators.

Observational programs are presently in progress to link the ultraviolet and optical flux calibrations and to provide a matching absolute calibration of the traditional Johnson-Cousins *UBVRI* system (e.g., Landolt 1973 and 1983). *The resulting flux calibration from 1150 to 10000 Å will thus be traceable, but not necessarily identical, to the IUE system in the UV (Bohlin 1986) and the AB79 system in the optical (Oke and Gunn 1983).*

Filter observations on HST will be reported as instrumental magnitudes on an absolute energy basis, i.e., without any colour corrections and with a zero-point coupled to the HST absolute flux system through a procedure introduced by Code *et al.* (1980).

In the following we provide more details.

Standard Stars

The primary HST standards on the optical list include cool DC white dwarfs selected because of their very smooth optical continua and sdO stars because of their usefulness in the blue. Their visual brightnesses range from $V = 11 - 16$ mag. Absolute fluxes for these stars are currently being derived by J. B. Oke using the Double Spectrograph (CCD) on the Palomar 5-m in a program which includes the metal poor sdF *AB*79 standards (Oke and Gunn 1983). Thus absolute fluxes for the HST primary standards will be traceable to the fluxes of the *AB*79 standards, which in turn are traceable to the Hayes and Latham (1975) calibration of Vega.

The primary HST standards on the UV list are hot blue stars which range from $V = 7 - 15$ mag. Observations of these stars are currently being obtained by R. C. Bohlin and others using IUE. The absolute fluxes thereby obtained are relative to the network of five standards that have been followed throughout the history of IUE (Bohlin 1986), and were originally calibrated relative to η UMa (Bohlin *et al.* 1980 and Bohlin and Holm 1980).

It can be expected from previous experience that continuity between the optical and UV standard absolute fluxes will be better than 5 %, with statistical errors typically less than 1-2% per 8-12 Å resolution element in the optical and about 3% per 25 Å bin in the UV.

The primary standards have been selected to be directly useful for the calibration of several instrument modes. Additional secondary standards are needed, however, for the bulk of the calibrations. As described by Koornneef *et al.* (1984)

and Bohlin *et al.* (1984), a total of more than a hundred targets will be required. Observations on the Johnson-Cousins *UBVRI* system by Landolt will be used to extend the HST photometric system to the faint magnitude levels required for some calibrations. His data will also be crucial for developing a better understanding of the relationship between the properties of specific HST magnitudes and the standard *UBVRI* system. Relative spectrophotometric data on most of the brighter secondary targets will be provided by R. Stone, and by S. Tapia and J. Liebert. Redundancy in the data-sets supplied by different observers is guaranteed by the inclusion of common targets. The resulting optical spectrophotometric standard list contains stars ranging from $V = 9 - 16$ mag, whereas the photometric stars must go as faint as the 21st mag to meet the FOC requirements. The total UV list contains mostly blue stars with $V = 0 - 15$ mag. The brightest of the UV stars are primarily relevant for the calibration of the HRS and HSP.

Absolute Fluxes and Magnitudes

In order to take advantage of both the traditional magnitude convention and the expected ability of HST to routinely measure precise fluxes, HST photometric measurements will be reported both in the language of absolute fluxes and as magnitudes. The HST fluxes will be relative to the absolute fluxes of the HST primary spectrophotometric standards. If the fluxes assigned to these standards are revised, absolute fluxes derived from HST measurements will also need to be revised. However, once the HST magnitudes of the standard stars for the various SIs are firmly established by actual HST measurements, no zero-point changes will be allowed. The HST photometric system thus provides stable magnitudes, but still allows for the derivation of absolute fluxes using the most current absolute calibration.

We now examine the explicit relations that are needed to calibrate broadband filter photometry and spectrophotometry in a uniform manner.

The most basic definition is that of the mean flux density as given by

$$f_\lambda(P) \equiv \frac{\int f_\lambda(\lambda) P(\lambda) \lambda d\lambda}{\int P(\lambda) \lambda d\lambda},$$

where $f_\lambda(\lambda)$ is the flux distribution of the star, usually in $erg\ cm^{-2}\ s^{-1}\ \AA^{-1}$, and $P(\lambda)$ is the dimensionless passband throughput function, giving the probability that a photon entering the telescope with wavelength λ will be recorded. The integrals are over the entire passband. The $P(\lambda)\lambda d\lambda$ weighting in the integrals is appropriate for photon-counting detectors as it ensures that the mean flux density is proportional to the detected photon count rate (e.g., Schneider *et al.* 1983).

The fundamental measurement made by HST detectors can be considered equivalent to a photon count rate, C. If U_λ is the flux density required to produce a unit response of one count per second in the passband, the measured absolute flux density is

$$f_\lambda(P) = U_\lambda(P) C.$$

The passband inverse sensititivity $U_\lambda(P)$ will initially be determined from the

https://doi.org/10.1017/S153929960000736X Published online by Cambridge University Press

calculated passband functions and the Optical Telescope Assembly (OTA) collecting area and will be corrected after launch by observing photometric standard stars.

Corresponding HST magnitudes will simply be

$$m_\lambda(P) = -2.5 \log U_\lambda(P) C + K,$$

where, initially, $K = -21.10$ (for U_λ in the units *erg* $cm^{-2}\mathring{A}^{-1}$). This choice of K causes $m_\lambda(5500\mathring{A})$ to be approximately equal to the Johnson V magnitude (e.g., Code *et al.* 1980). The zero-point K will initially be the same at all wavelengths, but must be permitted to vary slightly with time and wavelength in order to maintain a stable magnitude system. For example, K would need to be revised if the fluxes assigned to the *primary* spectrophotometric standard stars would undergo a systematic change. Changes in the filters through cumulative radiation damage or other causes might influence the value of their effective wavelength and/or K. Provided that these changes can be effectively tracked as a function of time, the stability of the HST photometric system can be ensured.

Detailed HST passband information will become available through the STScI, but as a convenience to observers and for consistency in the reporting of results, we will provide for each passband a characteristic wavelength, $\lambda_p(P)$, which we will refer to as the *pivot-wavelength*. This parameter is source-independent and defined as

$$\lambda_p(P) \equiv \sqrt{\frac{c f_\nu(P)}{f_\lambda(P)}} = \sqrt{\frac{\int P(\lambda)\lambda d\lambda}{\int P(\lambda) d\lambda/\lambda}}.$$

We have chosen the pivot-wavelength because it allows an exact conversion between the broadband flux densities $f_\nu(P)$ and $f_\lambda(P)$, as explained below. Of course, for any non-zero passband width, the pivot-wavelength differs somewhat from the more traditional *mean wavelength*,

$$\lambda_0 \equiv \frac{\int \lambda P(\lambda) d\lambda}{\int P(\lambda) d\lambda},$$

which is also source-independent. For a broad passband such as the Johnson V, λ_p is smaller than λ_0 by ~ 12 $\mathring{A}$ (see Table I).

The effective wavelength is an ill defined concept for any filter of finite width (e.g., Golay 1974; Schneider *et al.* 1983), but it is useful to define a *source dependent* passband parameter which can be used to estimate *shifts* of the effective wavelength with source characteristics (e.g., temperature, reddening, redshift). We will reserve the term *effective wavelength* for the mean wavelength of the detected photons,

$$\lambda_{eff} \equiv \frac{\int \lambda f_\lambda(\lambda) P(\lambda) \lambda d\lambda}{\int f_\lambda(\lambda) P(\lambda) \lambda d\lambda}.$$

As a measure of the *width* of a passband we will use

$$\lambda_{rms} \equiv \sqrt{\frac{\int (\lambda - \lambda_0)^2 P(\lambda) d\lambda}{\int P(\lambda) d\lambda}}.$$

https://doi.org/10.1017/S153929960000736X Published online by Cambridge University Press

The HST magnitude system, based on f_λ, can be converted to an analogous f_ν (in $erg\ cm^{-2}s^{-1}Hz^{-1}$) system defined by

$$f_\nu(P) \equiv \frac{\int f_\nu(\lambda)P(\lambda)d\lambda/\lambda}{\int P(\lambda)d\lambda/\lambda},$$

by calculating

$$m_\nu(P) = m_\lambda(P) - 5\log\lambda_p(P) + 18.70,$$

where $\lambda_p(P)$ is the pivot-wavelength in Å; m_ν will then be approximately equal to AB_ν from the ground-based optical $AB79$ system of Oke and Gunn (1983). It is important to use the pivot-wavelength when making this conversion, since a 1 % wavelength error would cause a 5 % error in the converted broadband flux.

Table I: Parameters, expressed in Å, of various passbands.

	Johnson			WFPC			FOC			HSP		
	U	B	V	336W	439W	569W	342W	430W	480LP	355M	450W	551W
λ_p	3646	4402	5493	3366	4363	5638	3392	4145	5348	3585	4363	5379
λ_0	3652	4417	5505	3371	4368	5652	3399	4156	5364	3590	4387	5397
λ_{rms}	202	362	367	171	215	414	221	311	423	190	456	420
$\lambda_{eff}(O8V)$	3623	4344	5442	3349	4340	5573	3363	4101	5282	3566	4268	5298
$\lambda_{eff}(M0V)$	3712	4606	5606	3414	4465	5760	3474	4371	5504	3675	4668	5523

3. THE SYNTHESIS OF CALIBRATION TARGET DATA

Well in excess of a hundred targets are involved in the first-order calibration, including linearity checks, of the HST SIs. Through observational programs and literature searches, data are being collected for each of the calibration targets.

For the primary spectrophotometric standards we will construct flux distributions by combining ultraviolet data from IUE and optical data by J. B. Oke to cover the wavelength range from 1150 to 10000 Å in a continuous manner. These absolute flux data will be directly applicable to the calibration of the spectrophotometric modes, and will be applied to the photometric modes by means of synthetic photometry using the formalism developed in Section 2.

The preparation of calibration data for the HST spectrographs is straightforward because mismatches between the spectral resolution of the calibration target flux-data and the instrumental resolution can be smoothed out. However, synthetic photometry will necessarily play a central role in calibrating those instrument modes which use photometric filters, because *no observational data through HST specific passbands* will be available before launch, except through a ground-based program under the direction of W. A. Baum, who is using replicas of a subset of the WFPC flight-filters. HST magnitudes for the broadband modes will therefore be *calculated*, taking full advantage of the *a priori* knowledge of the HST passbands.

https://doi.org/10.1017/S153929960000736X Published online by Cambridge University Press

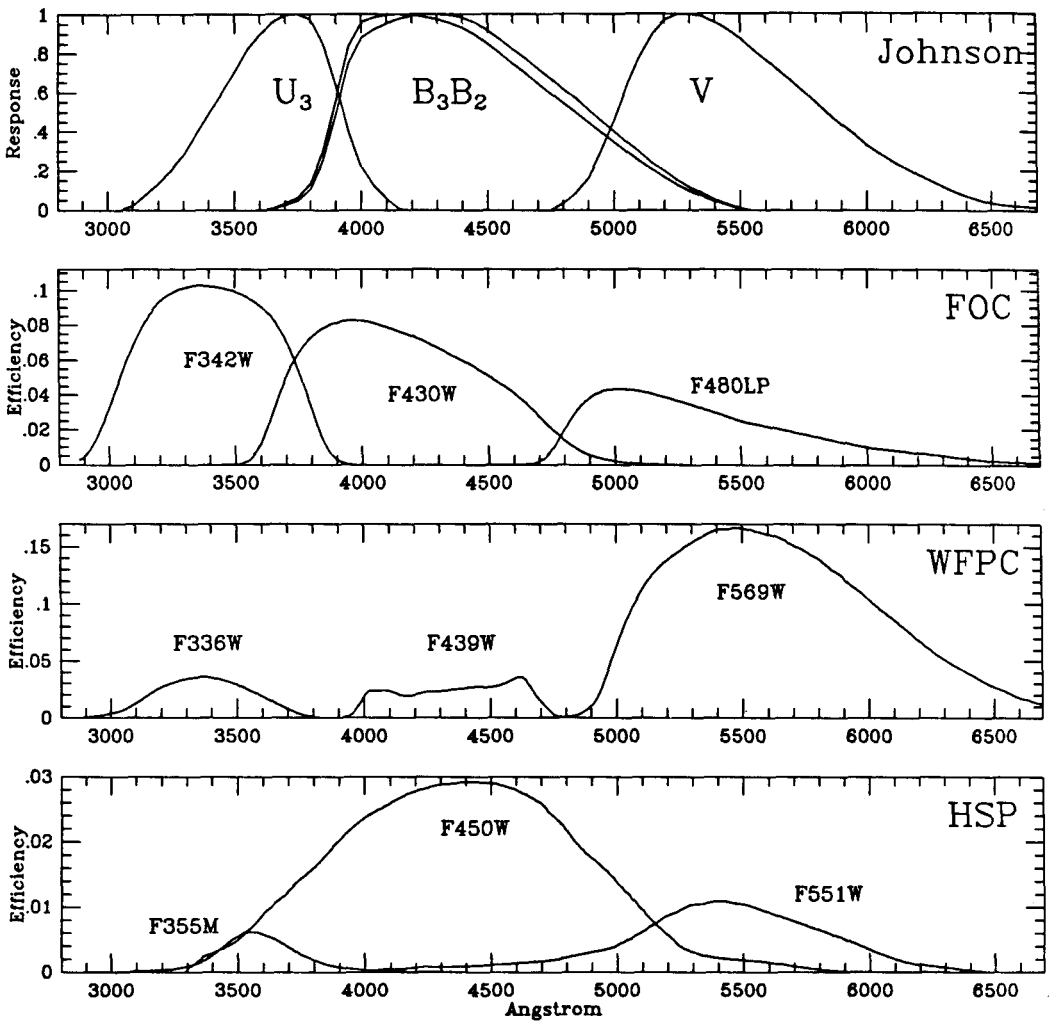

Figure 1. Effective passbands for a selected set of photometric filters. The first panel shows the normalized responses derived for the Johnson $U_3B_3B_2V$ passbands as given by Buser (1978). The remaining panels give throughput functions for those passbands on the various HST SIs which most closely resemble the Johnson passbands. The HST passbands are derived from the individual component throughput functions and the detector performance data provided by the Investigation Definition Teams. This information is the basic input for the instrument simulators which are being developed by the Instrument Support Branch at the STScI. The curves shown here were generated by these simulators. Note that the efficiencies given are 'best-estimate' pre-launch values only. The quantum efficiency curve used for WFPC did not include the effects of UV-flooding.

The shapes of photometric passbands of the HST SIs are very well determined since characteristic curves for all the components in the optical train have been obtained by the Investigation Definition Teams (IDTs) and the team responsible for the OTA. In collaboration with the Space Telescope European Coordinating Facility (STECF) in Munich, all this information is being collected and will become

https://doi.org/10.1017/S153929960000736X Published online by Cambridge University Press

available in a homogeneous format. From the data on the individual components, the overall passbands can be easily calculated.

In order to calculate HST magnitudes by use of synthetic photometry, flux-calibrated spectra on the HST photometric system are required in addition to the passband information. Such data will be obtained by launch in a few cases but spectrophotometry will not be available for many of the calibration targets. For example, a large number of photometric modes on the WFPC will be standardized using a set of 15th magnitude horizontal branch stars in ω Cen. We expect to acquire Johnson *UBV* photometric data for these stars, but will need to generate magnitudes on the HST system corresponding to the actual WFPC passbands. We show in Section 4 that the traditional linear colour equations do not suffice to transform the Johnson *UBV* data to the HST system, even for the most favourable cases of the *UBV* analogs on WFPC, FOC, and HSP.

When an observed absolute flux distribution is not available, we will make use of, for example, *UBVRI* measurements and an uncalibrated spectrum of the target or some idea of its spectral type. A best estimate of the absolute energy distribution for the target will be generated by 'tweaking' the relative spectrophotometry, or an appropriate stellar model, in such a way that integrations of the energy distribution over the *UBVRI* passbands conforms to the observational data. HST magnitudes can then be synthesized from the best fit energy distribution and the appropriate SI throughput functions. To achieve internal consistency, we will need to recalibrate the absolute fluxes for zero-magnitude of the *UBVRI* system to conform to the HST photometric system. This calibration will be based on *UBVRI* observations by A. U. Landolt of the *primary* spectrophotometric standards and the Johnson-Cousins passbands by Buser (1978).

4. SYNTHETIC TWO-COLOUR DIAGRAMS

Although some of the passbands on HST might eventually establish a standard in their own right, scientific continuity will often require the comparison of observations obtained through HST passbands with those obtained on standard systems. The Johnson *UBV* system provides an especially relevant example, as several of the IDTs have chosen to implement *UBV* analogs in their instrument on HST. Figure 1 illustrates the overall efficiencies for those photometric passbands aboard HST which most closely approximate the Johnson system. The passband parameters defined in Section 2 are given for each of these filters in Table 1. These passbands were used along with the library of stellar flux distributions by Straizys and Sviderskiene (1972) to generate the two-colour plots shown in Figure 2. These diagrams predict the behavior of a wide variety of stellar types observed with different instrument configurations available with HST.

While there is apparently a high degree of similarity between the HST systems and the standard *UBV*, the following differences can be pointed out.

(i) The zero point for the HST system is set by an imaginary source with constant f_λ rather than by the traditional *A0V* spectrum. This difference causes a

https://doi.org/10.1017/S153929960000736X Published online by Cambridge University Press

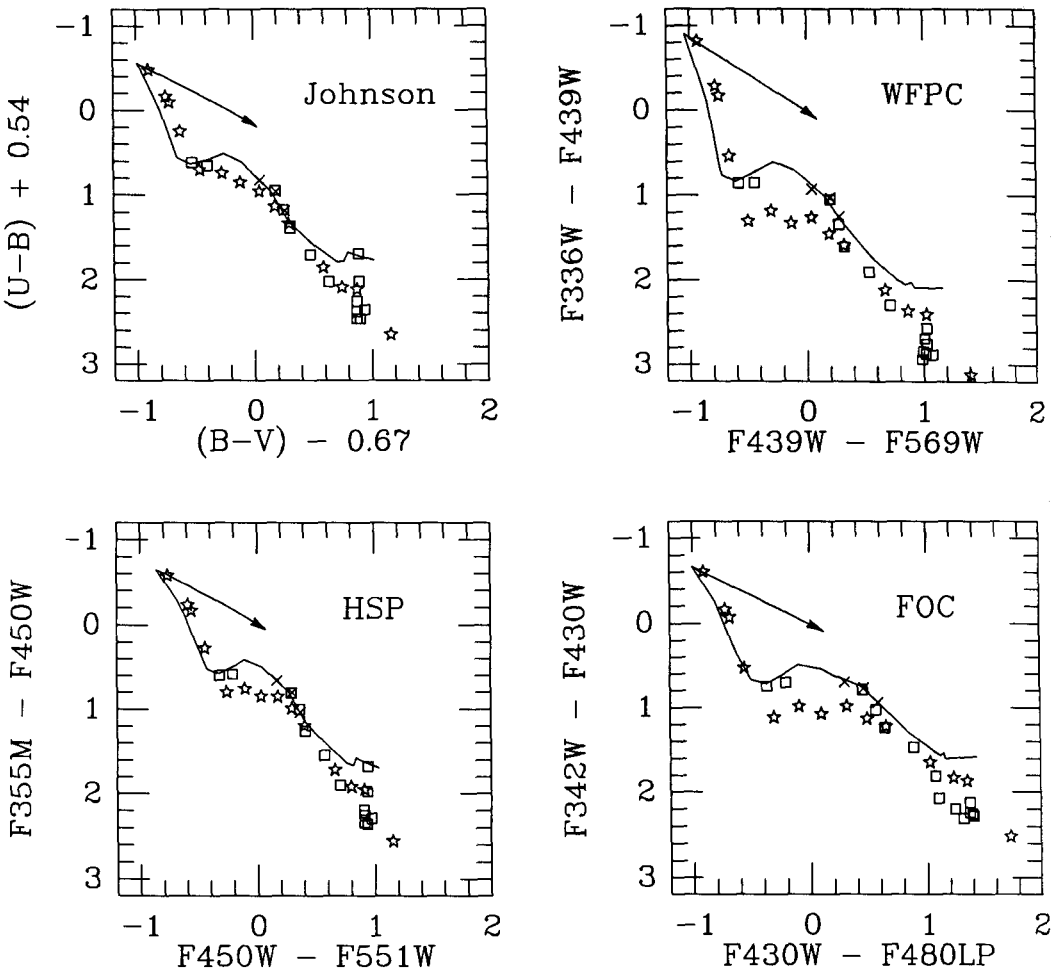

Figure 2. Synthetic two-colour diagrams for a selected set of filters. As in Figure 1, the first panel refers to the standard Johnson filters and simulates the $(U-B)$,$(B-V)$ diagram. The energy distributions used are those from Straizys and Sviderskiene (1972). The remaining panels give a similar diagram for the three SIs on HST which provide photometric capabilities with broadband filter modes. The solid line represents the main sequence, ⋆'s are used for supergiants, and ×'s and □'s denote subgiants and giants, respectively. The reddening vector corresponds to $E_{B-V} = 1$.

shift of approximately −0.54 in $(U-B)$ and +0.67 in $(B-V)$.

(ii) The ultraviolet passbands of the WFPC and FOC sample more light at shorter wavelengths than the Johnson U. This causes their $(U-B)$ analogs to be more sensitive to the UV depression shortward of $\lambda 4500$, which distinguishes intermediate- and later-type evolved stars from the main sequence.

(iii) Bandwidth effects produce curvature of the O-star reddening line shown in each of the two-colour diagrams. The initial reddening vector slopes are 0.69 for Johnson, 0.88 for WFPC, 0.68 for HSP and 0.66 for FOC. Note also that the

https://doi.org/10.1017/S153929960000736X Published online by Cambridge University Press

lengths of the reddening vectors differ appreciably among the various systems.

The deviations of the HST photometric systems from the standard *UBV* are shown in greater detail in Figure 3, where the differences between the Johnson colour indices and their HST analogs are plotted against $(U-B)$ and $(B-V)$, respectively. It is immediately evident that simple colour equations cannot be used to convert HST observations to the Johnson *UBV* system without introducing significant errors. This underlines the importance of synthetic photometry in the interpretation of HST measurements.

5. CONCLUSION

We have outlined a plan relying heavily on synthetic photometry techniques to deal effectively with the complexity of calibrating the multiple modes of HST. Absolute energy distributions will be observed or generated for all calibration targets, including those to be used for photometric calibration only. Instrumental magnitudes for the HST specific passbands will be calculated from these energy distributions. Cross-calibration of the various SIs is ensured, since the flux distributions will all be traceable to the primary standards. This coordinated approach to calibration, while requiring some pre-launch effort, will greatly reduce the amount of on-orbit calibration time. It is nevertheless anticipated that only a set of so-called 'core-modes' can initially be fully calibrated.

The ability to accurately predict the HST response to classes of objects not specifically included as calibration targets results in important savings of HST observing time. Only for a few 'workhorse' HST passbands, will it be possible to generate *empirical* standard star sequences covering a range in astrophysical parameters such as temperature, luminosity, chemical composition and reddening, from HST observations. Accurate synthetic photometry ultimately depends on our knowledge of the passbands. An observational program to verify the pre-launch passband functions would require prohibitive amounts of observing time. However, each calibration observation, if defined as the difference between the predicted and observed HST response, will provide information on the adequacy of the adopted passbands.

The calibration should give absolute photometric accuracies of a percent or two in the optical and ten percent in the ultraviolet. This accuracy is limited by uncertainties in the primary standard flux distributions and should be sufficient for most science presently anticipated. Reproducibility is expected to be much higher, and will ultimately be limited by the photometric stability of the SIs. Information on this will require the analysis of HST measurements from space.

The parameters a General Observer should expect to deal with in reducing an HST photometric or spectrophotometric observation are: the detected count rate C, the associated calibration parameters U_λ, K, and the pivot-wavelength λ_p. With this information and the relations given in Section 2, the HST observer can convert both photometric and spectrophotometric data to (broadband) flux densities f_λ, f_ν, or to the associated magnitudes m_λ and m_ν.

https://doi.org/10.1017/S153929960000736X Published online by Cambridge University Press

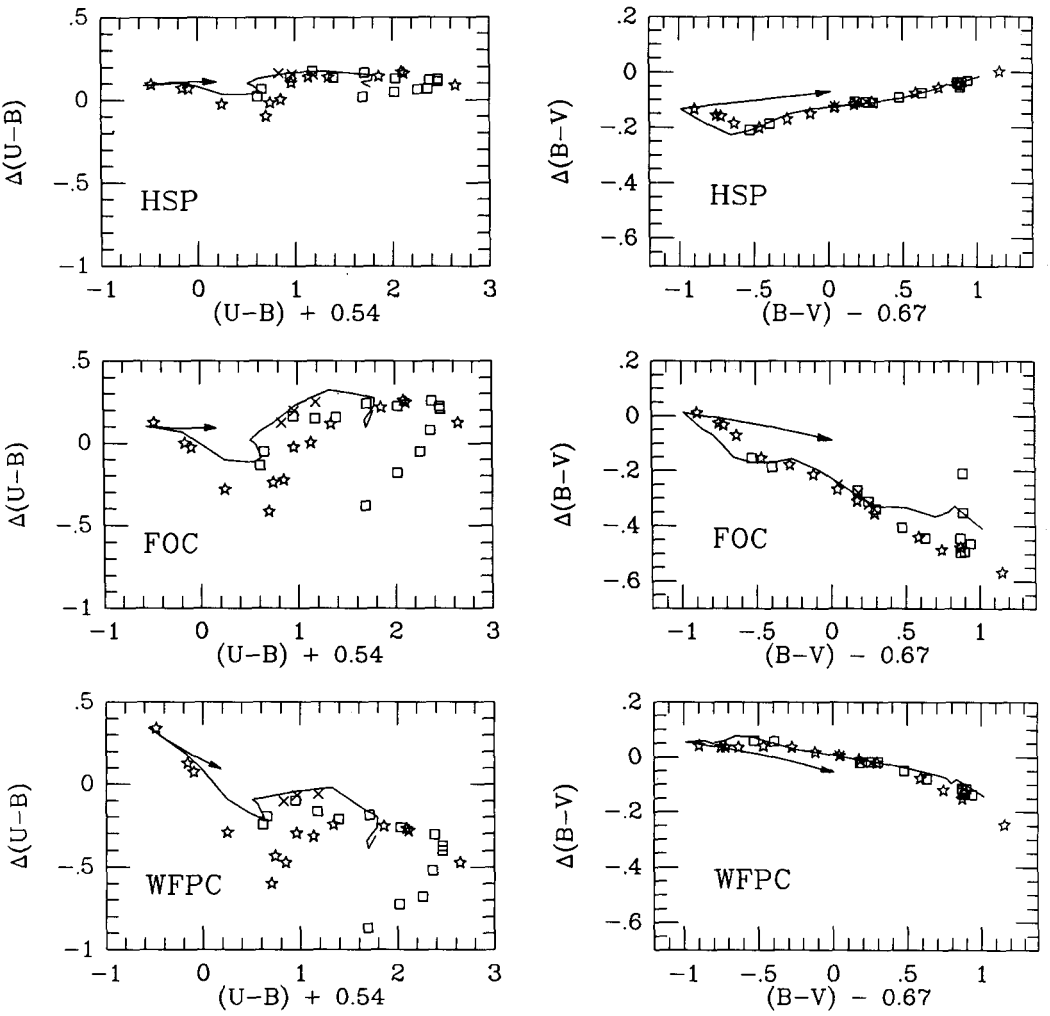

Figure 3. Differential two-colour diagrams. The present figure further illustrates how observations on the '*UBV* analogous' systems on HST are predicted to differ from the Johnson system. The data shown are derived from the data of Figure 2 by taking the difference between the standard $(U-B)$ and the SI-specific $(U-B)$ analogs for each of the three SIs under consideration as a function of $(U-B)$ (the three panels on the left hand side). Similarly, the three panels on the right hand side show the differences of the standard $(B-V)$ and the SI-specific $(B-V)$'s plotted as a function of $(B-V)$. As in Figure 2, the solid line represents the main sequence, ⋆'s are used for supergiants, and ×'s and □'s denote subgiants and giants respectively. The differential reddening line corresponding to $E_{B-V}=1$ is also shown.

ACKNOWLEDGEMENTS

The approach to the calibration of HST reported here is the result of inputs from many individuals. In particular we like to mention numerous discussions and consultations with Bill Baum, Art Code, Ivan King, Arlo Landolt, and Bev Oke,

who generously made their collective decades of calibration experience available. We would also like to mention the fruitful collaboration with the IDTs and the STScI instrument scientists. The data on the HSP passbands used in Section 4 were provided by Rick White. Shawn Ewald ran the FOC and WFPC simulators to provide similar information for those SIs. We are grateful to Dorothy Schlogel for help in preparing the manuscript. R. Buser acknowledges the support of the National Aeronautics and Space Administration for his stay in Baltimore as well as partial support through the Swiss National Science Foundation.

References

Bohlin, R.C. 1986, *Astrophys. J.* (submitted).

Bohlin, R.C., Blades, J.C., Holm, A.V., Savage, B.D., and Wu, C.-C. 1984,'Standard Astronomical Sources for ST: 1. *UV Spectrophotometric Standards*'.

Bohlin, R.C., Holm, A.V., Savage, B.D., Snijders, M.A.J., and Sparks, W.M. 1980, *Astron. Astrophys.* **85**, 1.

Bohlin, R.C. and Holm, A.V. 1980,*NASA IUE Newsletter* **10**, 37; 1981, *ESA IUE Newsletter*, **11**, 18.

Buser, R. 1978, *Astron. Astrophys.* **62**, 411.

Code, A. D., Holm, A. V., and Bottemiller, R. L. 1980, *Astrophys. J. Suppl.* **43**, 501.

Golay, M. 1974, *Introduction to Astronomical Photometry*, D. Reidel Publ. Comp., Dordrecht-Boston, pp. 39*ff*.

Hayes, D.S. and Latham, D.W. 1975, *Astrophys. J.* **197**, 593.

Koornneef, J., Baum, W.A., Bohlin, R.C., Dolan, J., Oke, J.B., and Turnshek, D.A. 1984, 'Report of the *Optical Calibration Target Working Group*'.

Landolt, A.U. 1973, *Astron. J.* **78**, 959.

Landolt, A.U. 1983, *Astron. J.* **88**, 439.

Oke, J.B. and Gunn, J.E. 1983, *Astrophys. J.* **266**, 713.

Schneider, D.P., Gunn, J.E., and Hoessel, J.G. 1983, *Astrophys. J.* **264**, 337.

Straizys, V. and Sviderskiene, Z. 1972, *Bull. Vilnius Astron. Obs.* **35**.